

Surface roughening of Ge(001) during 200 eV Xe ion bombardment and Ge molecular beam epitaxy

E. Chason, J. Y. Tsao, K. M. Horn, S. T. Picraux, and H. A. Atwater^{a)}

Sandia National Laboratories, Albuquerque, New Mexico 87185

(Received 1 September 1989; accepted 30 October 1989)

The kinetics of surface roughening of Ge(001) during 200 eV Xe ion bombardment and during Ge molecular beam epitaxy (MBE) are studied by real-time reflection high-energy electron diffraction. In both cases, initially smooth surfaces reach a steady state roughness which depends on temperature and incident ion or adatom flux. The data are analyzed in terms of a phenomenological model in which beam-induced roughening competes with beam-induced smoothening, and in which the defect creation rate and surface diffusivity are fitting parameters. For comparable fluxes, the temperature dependences for the net roughening induced by ions and adatoms are strikingly similar, implying a similarity in the surface diffusivities of vacancies and adatoms. For the case of ion-induced roughening, approximately one surface defect (in units of displaced surface atoms) is created per ion which is consistent with calculations assuming that a large fraction of atomic displacements recombine without producing surface defects at these ion energies.

I. INTRODUCTION

The evolution of surface morphology during surface processing depends in general on the migration and interaction of defects on the surface. In a previous work¹ we investigated the kinetics of roughening of Ge(001) during Ge molecular beam epitaxy (MBE) as a function of temperature. The roughening kinetics were interpreted in terms of a phenomenological model based on a competition between roughening processes (clustering of new adatoms) and smoothening processes (cluster annihilation by adatom-induced coalescence or ledge motion).

In this work, we extend that investigation to the kinetics of roughening of Ge(001) during low-energy (200 eV Xe) ion bombardment as a function of substrate temperature. In this case, the roughening is apparently not mediated by surface adatoms (positive defects) contributed by MBE, but primarily by surface vacancies (negative defects) contributed by low-energy ion bombardment. We believe this to be true on the basis of reflection high energy electron diffraction (RHEED) measurements of ion roughening followed by growth.² Ion-roughened surfaces smoothen in the presence of incoming adatoms, presumably by annihilation with an excess of surface vacancies produced by the ions.

Surface adatoms and surface vacancies have the same (but complementary) effect on static surface morphology: an isolated adatom introduces the same roughness to an otherwise smooth surface as does an isolated vacancy. However, the dynamic evolution of the surface morphology under a flux of adatoms or ions is determined by the migration and interaction of the surface defects they create. Surprisingly, the kinetics of ion beam roughening are remarkably similar to those of growth roughening, even though the primary defects are surface vacancies in one case and surface adatoms in the other case. This suggests a similarity in the way the two kinds of defects migrate and interact.

II. EXPERIMENTAL

The measurements were performed in an ultrahigh vacuum (UHV) growth chamber with a base pressure of 1×10^{-9} Torr. During ion bombardment, the chamber was backfilled with Xe to a pressure of 5×10^{-5} Torr. The 4×6 mm² sample was prepared by sequential pad polishes in Br: methanol and methanol.³ A thin (1000 Å) layer of Si was evaporated onto the backside of the sample to ensure good wetting by In, which was used to attach the sample to the sample holder.

The surface morphology was measured by *in situ* RHEED using a computer-controlled video acquisition system. Measurements were made of the specular beam intensity in the out-of-phase condition⁴ between the (004) and (008) bulk diffraction peaks, at an azimuthal angle of ~ 8 deg away from the [001] direction. The electron gun was operated at 20 keV. A nonzero base line was subtracted from each measured line shape to remove background intensity not associated with any particular diffraction feature.

We interpret our RHEED intensity measurements in terms of the kinetic approximation described in Ref. 4, which neglects the effects of multiple scattering when the diffraction geometry is chosen appropriately. The analytical expression relating the specular RHEED intensity to the roughness of a surface created by purely statistical deposition of θ monolayers is given in Sec. V. In this static diffraction condition, our experience is that RHEED is sensitive to roughness in general but cannot distinguish between two level and multilevel roughness. However, from measurements at high symmetry azimuths and other tilt angles, we believe the roughnesses measured here to be predominantly two level. Indeed, for all the measurements discussed here, "spotty" patterns characteristic of extremely rough surfaces were never observed even from surfaces roughened to the point where the intensity of the diffracted beam was nearly elimin-

ated. Since our samples, as-received, were miscut from the [001] surface by $\sim 1/4$ – $1/2$ deg, the lateral scale of the clusters contributing to surface roughness must be less than the mean terrace length of 170–340 Å.

The ion source was a Physical Electronics electron impact sputter gun with a tungsten filament and independent acceleration and focusing electronics. The acceleration voltage was 200 V for all the measurements made in this work. The current on target was measured to be 1.0 and $0.67 \mu\text{A}/\text{cm}^2$ for the two sets of ion beam measurements described below, but since this measurement contains no correction for secondary electrons, it is only an estimate of the ion flux. Reproducibility in the ion flux is estimated to be within $\pm 30\%$ based on measurements of the current and profiling of the beam. The ions were incident on the sample at an angle of 60 deg from the surface normal at an azimuthal angle of approximately 37 deg relative to the [001] direction on the surface. The growth source was an effusion cell; a deposition rate of approximately 0.006 monolayers/s was used for the growth roughening measurements. During growth, pressures typically rose to $\sim 6 \times 10^{-9}$ Torr.

After being placed in the vacuum, a smooth sample surface was generated by ion beam sputtering for 50 minutes at 500 °C with a 300 eV Xe beam at a flux of $1.3 \mu\text{A}/\text{cm}^2$, and then annealing at 650 °C for 20 min. The resulting surface was smooth according to RHEED with a strong specular beam in the out-of-phase diffraction condition. After each ion roughening or growth measurement, the surface was annealed for 10 min at 650 °C which was sufficient to restore the intensity of the out-of-phase beam and hence to restore the original surface smoothness.

III. ION BEAM RESULTS

The ion beam roughening measurements were made by bombarding initially smooth surfaces with 200 eV Xe ions at fluxes of approximately 0.01 monolayers/s ($1.0 \mu\text{A}/\text{cm}^2$) and 0.007 monolayers/s ($0.67 \mu\text{A}/\text{cm}^2$) relative to 6.24×10^{14} surface atoms/ cm^2 -monolayer for Ge (001). The decrease in RHEED intensity (normalized to the starting intensity) for an incident Xe flux of $1.0 \mu\text{A}/\text{cm}^2$ is shown in Fig. 1(a) at various temperatures. The surfaces do not roughen without bound, but reach a temperature dependent steady-state roughness. For temperatures above 300 °C, the degree of roughening was too small to measure within the stability limits of our RHEED acquisition system. For temperatures below 200 °C (not shown), the surface became so rough that the RHEED intensity went to zero within our detection capability. The ion roughening measurements made with the lower incident beam flux of $0.67 \mu\text{A}/\text{cm}^2$ exhibit a similar time dependence but with a shift to lower temperatures for the same degree of steady state roughness.

IV. GROWTH RESULTS

Measurements of growth roughening performed on the same sample are shown in Fig. 1(b) for comparison with ion beam roughening. The temperature dependence of the growth roughening is similar to that of the ion beam rough-

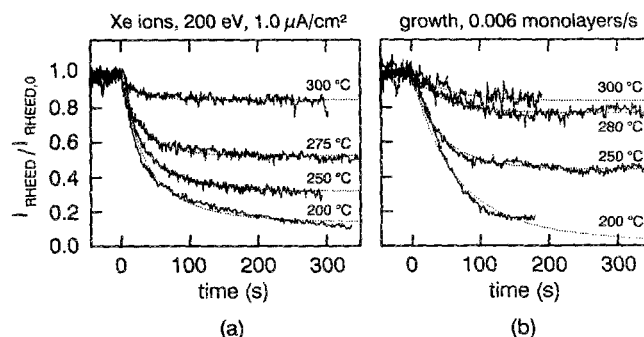


FIG. 1. The normalized RHEED intensity for the Ge(001) surface at the indicated temperature during (a) 200 eV Xe ion bombardment at $1.0 \mu\text{A}/\text{cm}^2$, and (b) Ge MBE at 0.006 monolayers/s. Dotted lines represent fits to the data, as described in the text.

ening, in both the steady-state roughness and the rate of roughening.

The maximum measured temperature at which these surfaces roughen during growth is somewhat lower than that published in our previous work.¹ Differences between the growth rates used in the two experiments account for the difference as explained in the following section.

V. PHENOMENOLOGICAL MODEL OF DEFECT-INDUCED ROUGHENING AND SMOOTHENING

Since the kinetics of ion beam roughening and growth roughening are so similar, it is straightforward to interpret them both in terms of our previous phenomenological model for growth roughening. That model involves a competition between roughening (by defect migration and nucleation of stable two-dimensional clusters) and smoothening (by the annihilation of clusters by defect-induced cluster coalescence via ledge motion). Thus, the roughening/smoothening process is mediated by the kinetics of surface defect migration and incorporation. In the case of the ion beam roughening, the fundamental surface defect involved is presumed to be predominantly vacancy-like, while in the case of growth the defects are presumed to be adatoms.² The balance between roughening and smoothening is determined by the substrate temperature, with greater defect mobility at higher temperatures contributing to less roughening, as shown in Figs. 1(a) and 1(b). The regime of the present measurements is believed to be characterized by less than an atomic layer of net roughness, i.e., still relatively smooth surfaces on a macroscopic scale.

In our earlier work,¹ we described the decrease in the RHEED intensity associated with the deposition of θ monolayers if the layer occupation is described by a Poisson distribution. For this simple case of statistical growth, the normalized RHEED intensity ($I_{\text{RHEED}}/I_{\text{RHEED},0}$) is described by

$$I_{\text{RHEED}}/I_{\text{RHEED},0} = e^{-\theta} \quad (1)$$

From this expression, we associate mathematically the normalized RHEED intensity with an equivalent coverage, θ_{eq} , which if distributed statistically would give such a RHEED intensity. At low temperature, the rate of roughening is

equal to the deposition rate ($\dot{\theta}_{eq} = \dot{\theta}$) and the form in Eq. (1) is found to fit the growth roughening data quite well. For the relatively low equivalent coverages involved in this experiment, Eq. (1) is in fact an adequate approximation to the RHEED intensity whether the layer coverage is distributed statistically or confined to only two layers. To understand the temperature dependence of the roughening, a rate equation expressing the kinetic balance between roughening and smoothening was developed for θ_{eq} :

$$\dot{\theta}_{eq} = j \left[\frac{j}{j + D/l^2} \right] - 4j \left[\frac{D/l^2}{j + D/l^2} \right] \theta_{eq} \quad (2)$$

where j is the rate of defect production at the surface (measured in monolayers/s), and D/l^2 is the rate at which defects annihilate at sinks of roughness spaced approximately by l . The first term in this equation is a roughening term, corresponding to the rate of roughening in the presence of diffusion. The factor $j/[j + (D/l^2)]$ represents the balance between the number of defects which cluster or otherwise remain on the surface and contribute to new roughness relative to those which are annihilated at sinks such as terrace ledges. At low temperature (where diffusion is negligible) this factor is unity and the roughening rate is identical to the growth rate. As diffusion becomes more significant, the roughening rate decreases.

The second term in Eq. (2) represents the effect of beam-induced smoothening by diffusion of defects. This smoothening is enhanced at higher temperature, to reflect our expectation that the growth mode transforms from cluster nucleation and coalescence to the propagation of terrace ledges. This model is described in more detail elsewhere,¹ along with analysis of the error incurred by assuming the surface roughness obeys a Poisson distribution.

VI. ANALYSIS OF RESULTS

The two parameters j and D are obtained from nonlinear least-squares fitting of the RHEED intensity during roughening to the form in Eqs. (1) and (2). The dotted lines in Figs. 1(a) and 1(b) represent the result of that fitting. The value of the defect creation flux j was allowed to vary in each fit to reflect the variability in the ion gun and the deposition source. The fit values for the defect production fluxes are 0.011 ± 0.002 and 0.007 ± 0.003 monolayers/s for the two sets of ion roughening measurements and 0.006 ± 0.002 monolayers/s for growth.

The values for D/l^2 obtained from the two-parameter fit is shown in Fig. 2 for ion roughening (circles) and growth roughening (crosses), respectively versus inverse temperature. The open circles represent the results of roughening at $1.0 \mu\text{A}/\text{cm}^2$ while the filled circles represent the results at $0.67 \mu\text{A}/\text{cm}^2$. The full set of data is reasonably well fit by a straight line on the Arrhenius plots; the tendency of the data to deviate from a straight line at low temperature may be due to the greatly increased sensitivity to any error in the background subtraction from the measured RHEED intensity when the steady-state intensity is low. Alternatively, it may indicate that the temperature dependence is not purely Arrhenian or cannot be described by a single activation energy.

We recommend caution in extrapolating these results to lower temperatures where measurements have not yet been made.

There are no extra adjustable parameters used to fix the scale for D/l^2 ; thus it is significant that the data for two different ion fluxes and for growth as well as for ion bombardment all lie along the same line. The activation energy obtained from the fitting (0.83 ± 0.13 eV) is in the range of values reported for surface diffusion on other semiconductor surfaces⁵ and the prefactor D_0/l^2 [$1.3 \times 10^6 (\text{s}^{-1})$] is consistent with an annihilation rate of defects at terrace ledges spaced from 120 to 240 lattice sites apart (within the range estimated from the sample misorientation).

VII. DISCUSSION

The most striking result of the ion beam roughening is its similarity to the growth roughening in both the rate and steady-state roughness over the same temperature regime. Moreover, both types of roughening seem to be well described by the same simple model. Although we recognize that the model presented here is only a simplified first-order approach to the complex problem of surface dynamics, it does represent a useful starting point until a more thorough treatment can be developed. In our previous work,¹ we tentatively identified growth smoothening with terrace ledge motion mediated by diffusion of adatoms to those terrace ledges separated by a mean spacing of l . By analogy, we identify here ion beam smoothening with terrace ledge motion mediated by the diffusion of surface vacancies.

For ion smoothening to be effective, the ion-induced displacements must be confined to the near surface region. At higher ion energies, the ratio of bulk displacements to surface displacements increases and any modeling of surface disordering is expected to become more complex due to competing bulk disordering and multilayer erosion of the surface. Indeed, during ion beam roughening by 500 eV Ar ions at a flux of $0.3 \mu\text{A}/\text{cm}^2$, the surface did not reach a steady-state roughness but continued to roughen without bound

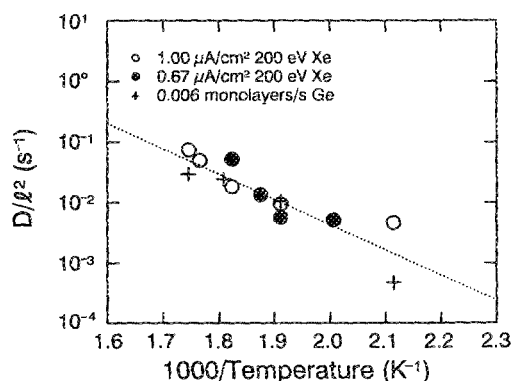


FIG. 2. Diffusivity of surface defects obtained from fitting temperature dependence of the roughening measurements for ion bombardment and MBE. Open circles: 200 eV Xe at $1.0 \mu\text{A}/\text{cm}^2$; solid circles: 200 eV Xe at $0.67 \mu\text{A}/\text{cm}^2$; crosses: growth at 0.006 monolayers/s. The dotted line represents a fit to an Arrhenius temperature dependence.

even at 600 °C. Burger and Reif,⁶ as well, observed significant subsurface damage from the bombardment of Si with 200 eV Ar ions. For 200 eV Xe on Ge, however, Monte Carlo calculations⁷ indicate that 80% of the atom displacements occur within the first three atomic layers of the sample which we consider to be the near surface region.

The number of defects created per incident ion or adatom can be obtained from the ratio of j to the measured flux for comparison with the results of our Monte Carlo calculations. For the case of growth roughening, this ratio is unity since each adatom contributes exactly one surface defect. This has been verified experimentally in earlier work¹ by comparison of the growth flux determined by a crystal growth monitor (0.025 monolayers/s) with the value obtained from the fit (0.023 ± 0.002 monolayers/s). For the ion roughening, the ratio of defect production to ion flux is 1 for both 0.01 monolayers/s and 0.007 monolayers/s. This value does not differentiate between roughening by the creation of adatoms or surface vacancies. Our calculation, based on a surface atom displacement threshold equal to half the bulk value (bulk displacement energy = 15 eV), gives 2.7 displacements per 200 eV Xe ion in the first three layers. Also, the calculated sputtering yield for these surface displacements is 20%; sputtering events contribute vacancies to the surface but not adatoms. Thus, in the limit of no vacancy-interstitial (surface vacancy-adatom) recombination, this calculation corresponds to 4.9 defects per Xe ion. In the opposite limit of 100% recombination prior to any contribution to roughening, only the excess vacancies of 0.5 per Xe would contribute. The experimentally determined value of about one defect per Xe is therefore between the calculated bounds and corresponds to a large amount ($\sim 90\%$) of recombination. This is clearly a different regime of ion damage than that typically used in ion sputtering. Earlier work by

Heinz *et al.*⁸ using 5 keV Ar on Si (111) surfaces determined a surface defect production rate of greater than 35 per ion.

The similarity between the diffusional kinetics of the ion-induced surface vacancies and adatoms suggests that the environment of adatoms on the surface and atoms surrounding a vacancy are energetically similar. Some possible configurations of adatoms and vacancies on the surface are shown schematically in Fig. 3. The atoms already in the surface are represented by open circles; the surface dimer bond is indicated by the bowed lines. Atoms below the surface are represented by small filled circles.

The "surface-bonded" adatom (represented by the solid circle in Fig. 3) is an adatom which has replaced a surface dimer and is bonded to two atoms in the layer below. As Gossman and Feldman have pointed out,⁹ in order for the adatom to become incorporated into the surface, it must first break the dimer bond at which point it increases its coordination. After the dimer bond is broken the atoms below move into their bulk lattice positions. This situation is energetically similar to that of the surface vacancy which is shown as a pair of dotted lines to represent the breaking of two bonds when the surface atom is removed. In both configurations migration requires the breaking of two bonds between a surface atom and the layer below it.

In contrast, the configuration referred to as the "free" adatom is represented by the crosshatched circle. As shown in the figure, it is only weakly bonded to the surface by a dangling bond. Its diffusional kinetics would be expected to be very different from the surface vacancy. The similarity of the ion roughening and growth roughening measurements suggests that this configuration is much shorter lived or less likely than the surface-bonded configuration.

The frequency of occurrence of the surface-bonded configuration for the adatom has been examined in molecular dynamics simulations by Brenner and Garrison.¹⁰ During the short (500 ps) duration of their simulation, they do, in fact, observe rapid replacement of the surface dimer with adatoms which previously occupied a dangling bond. They identify this configuration as the initiation of the next layer of epitaxial growth since the surface-bonded adatom is in a stable lattice site after this rearrangement. They do not report on the probability of this adatom reverting back to a free adatom or the motion of the surface bonded adatom during the simulation.

As a final comment, it is important to note that the ability to grow or ion bombard without roughening is very sensitive to the condition of the initial surface. It is our experience that the better the starting surface (cleaner, smoother, fewer defects) the lower the temperature at which it will stay smooth during growth or ion beam bombardment. Measurements done under poorer vacuum conditions exhibited ion beam roughening at temperatures as high as 600 °C for 200 eV Xe at $1.0 \mu\text{A}/\text{cm}^2$. Surfaces that have been prepared badly, e.g., by growth on a dirty surface, also roughen at higher temperatures. It is generally accepted that these types of surface imperfection can be covered by the growth of large buffer layers, and the growth of thick buffer layers prior to attempting to grow high-quality electronic structures is routine. However, relatively high temperatures are required to pre-

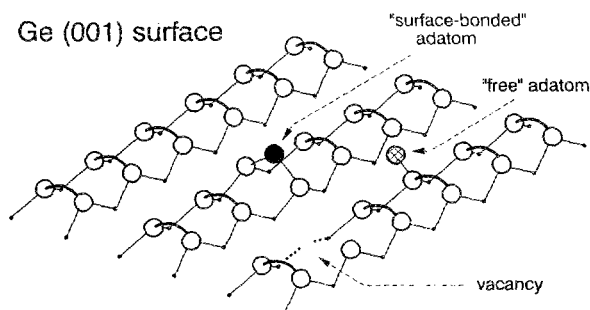


FIG. 3. Schematic representation of adatoms and vacancies on the Ge(001) 2×1 dimerized surface. Open circles represent surface atoms with the dimer bond represented by the thick line. The surface atoms are bonded to the layer below (represented by dots) by the thin lines. The weakly bonded surface adatom is represented by the crosshatched circle. The surface-bonded adatom, represented by the solid circle, has replaced the dimer bond and is doubly bonded to the atoms on the surface. The surface vacancy is represented by the broken bonds shown as dotted lines. Note that the coordination of the surface-bonded adatom is the same as for the atom adjacent to the surface vacancy.

vent disorder during growth, and this can make it difficult to fully bury all types of surface disorder and impurities. Alternatively, extremely low-energy ion bombardment of the type investigated here may lead to highly perfect and quite smooth substrates by exposing new unadulterated material if carried out at appropriate temperature(s) prior to epitaxy. We suggest this approach may be useful for initial surface preparation while avoiding the bulk disorder and possible gas trapping found at the much higher energies (≥ 1000 eV) typically associated with sputter cleaning. Of course lower ion energies than those used here, preferably below the bulk displacement threshold, would be even better for minimizing bulk damage.

VIII. CONCLUSIONS

Measurements of the kinetics of Ge(001) surface roughening by 200 eV Xe ion bombardment and by Ge deposition indicate that both can be modeled by the same rate equation expressing the balance between roughening and smoothening processes on the surface. In addition, the temperature dependence of these processes is observed to be the same. We interpret these results as indicating that the energetics of surface diffusion (~ 0.8 eV) for adatoms and surface vacancies are similar. This result implies the same coordination for adatoms and surface vacancies, suggesting that the adatom does not remain free on the surface, but instead becomes bonded in the place of the surface dimer. The observed surface defect production rate of about one defect per incident Xe ion is consistent with our calculations of the displacement rate and suggests that a large fraction of the primary displacements recombine without contributing to surface defect production.

ACKNOWLEDGMENTS

We would like to acknowledge the technical assistance of Dan Buller and Richard Blake in construction and maintenance of the MBE chamber. One of the authors (H. A. Atwater) acknowledges the support of the Caltech Program in Advanced Technologies. This work performed at Sandia National Laboratories supported by the U.S. Department of Energy under Contract No. DE-ACO4-76DP00789.

- ^{a)} Permanent address: Thomas J. Watson Sr. Laboratory of Applied Physics, California Institute of Technology, Pasadena, CA 91125.
- ¹ E. Chason, J. Y. Tsao, K. M. Horn, and S. T. Picraux, *J. Vac. Sci. Technol. B* **7**, 332 (1989).
- ² E. Chason, K. M. Horn, J. Y. Tsao, and S. T. Picraux, *Mat. Res. Soc. Symp. Proc.* **128**, 35 (1989).
- ³ D. E. Aspnes and A. A. Studna, *Appl. Phys. Lett.* **39**, 316 (1981).
- ⁴ J. M. van Hove, P. R. Pukite, P. I. Cohen, and C. S. Lent, *J. Vac. Sci. Technol. A* **4**, 1251 (1986).
- ⁵ J. H. Neave, P. J. Dobson, B. A. Joyce, and J. Zhang, *Appl. Phys. Lett.* **47**, 100 (1985).
- ⁶ W. R. Burger and R. Reif, *J. Appl. Phys.* **62**, 4255 (1987).
- ⁷ S. T. Picraux, D. K. Brice, K. M. Horn, J. Y. Tsao, and E. Chason, *Proceedings of the 13th International Conference on Atomic Collisions in Solids*, Aarhus, Denmark, 1989; *Nucl. Instrum. Methods B* **48**, 414 (1990).
- ⁸ T. F. Heinz, M. M. T. Loy, and W. A. Thompson, *J. Vac. Sci. Technol. B* **3**, 1467 (1985).
- ⁹ H. J. Gossman and L. C. Feldman, *Phys. Rev. B* **32**, 6 (1985).
- ¹⁰ D. W. Brenner and B. J. Garrison, *Surf. Sci.* **198**, 151 (1988).